J. Fluid Mech. (1967), *vol.* 28, *part* 4, *pp.* 625–641
Printed in Great Britain

On vortex street wakes

By P. W. BEARMAN
Cambridge University Engineering Laboratory†

(Received 15 June 1966)

The flow in the wake of a two-dimensional blunt-trailing-edge body was investigated in the Reynolds number range, Reynolds number being referred to base height, $1{\cdot}3 \times 10^4$ to $4{\cdot}1 \times 10^4$. The effects of splitter plates and base bleed on the vortex street were examined. Measurements were made of the longitudinal spacing between vortices and the velocity of the vortices, and compared with values predicted by von Kármán's potential vortex street model. The lateral spacing was estimated by using both the von Kármán and Kronauer stability criteria. A new universal wake Strouhal number is devised, using the value of lateral spacing predicted by the Kronauer stability condition as the length dimension. A correlation of bluff-body data was found when pressure drag coefficient times Strouhal number was plotted against base pressure.

1. Introduction

The aim of this paper is to compare measured vortex street parameters with those predicted by existing theories and to investigate the validity of the vortex street stability criteria of von Kármán and Kronauer. It is also intended to investigate how vortex streets are affected by the introduction of either splitter plates or base bleed.

Von Kármán (see Milne-Thomson 1938) represented the vortex street wake which forms behind a bluff body by an idealized potential flow model consisting of a double row of staggered point vortices. The associated vortex street drag coefficient C_{DS} can be shown to equal

$$C_{DS} = \frac{4}{\pi}\left(\frac{U_S}{U_0}\right)^2\left[\coth^2\frac{\pi b}{a} + \left(\frac{U_0}{U_S} - 2\right)\frac{\pi b}{a}\coth\frac{\pi b}{a}\right], \tag{1}$$

where

$$C_{DS} = D_S/\tfrac{1}{2}\rho a U_0^2,$$

D_S is the vortex street drag, U_0 free-stream velocity, U_S is the velocity of vortices relative to the free stream, a the longitudinal spacing between vortices and b the lateral spacing between vortices. b/a is often referred to as the spacing ratio.

It has also been shown by von Kármán that vortex streets are stable to first-order disturbances if $b/a = 0{\cdot}281$. Substituting this value of the spacing ratio into (1) gives the von Kármán vortex street drag formula

$$C_{DSV} = 1{\cdot}583(U_S/U_0) - 0{\cdot}63(U_S/U_0)^2. \tag{2}$$

† Now at the National Physical Laboratory, Teddington, Middlesex.

C_{DSV} can be determined from measurements of the longitudinal vortex spacing and the vortex shedding frequency f. Since $af = U_N$, where U_N is the velocity of the vortices relative to the model, and $U_0 = U_N + U_S$,

$$\frac{U_S}{U_0} = 1 - \frac{fa}{U_0} = 1 - \frac{Sa}{h}, \tag{3}$$

where $S\ (=fh/U_0)$ is the Strouhal number. Conversely, knowing f and vortex street drag, both a and U_N can be predicted.

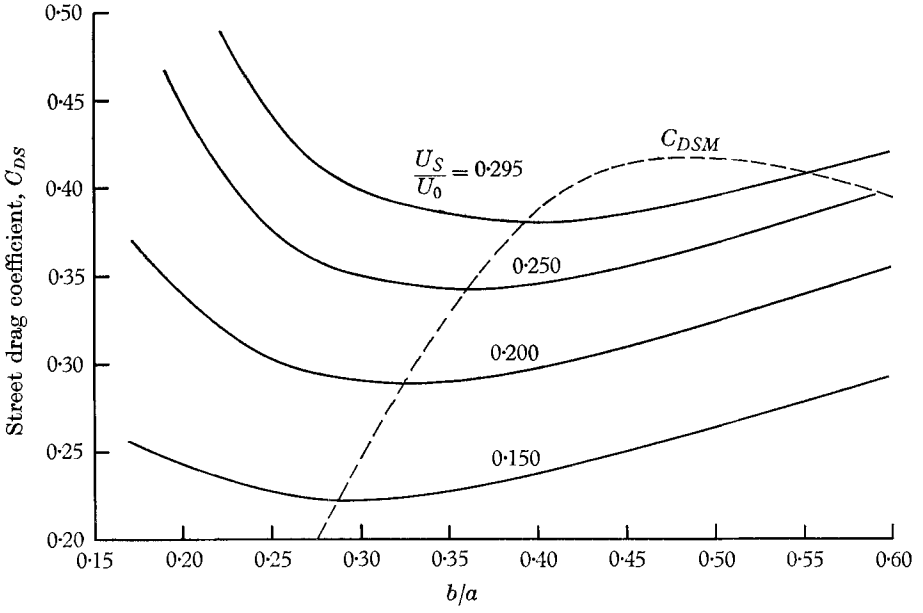

FIGURE 1. Vortex street drag coefficient versus spacing ratio for various values of vortex velocity.

In his review paper, Wille (1960) pointed out that any array of vortices is unstable to any order of disturbance higher than the first. The arrangement is particularly unstable to any three-dimensional disturbance. It would seem very unlikely, therefore, that vortex streets could possibly exist at high Reynolds numbers where the flow is fully or partly turbulent. The fact that vortex streets do exist casts suspicion on the von Kármán stability condition. Various authors, including Timme & Wille (1957) and Berger (1964), have measured values of b/a between 0·20 and 0·40 with b/a increasing with distance along the wake.

Kronauer (1964) has shown that spacing ratio is not an important parameter in determining C_{DS}. Figure 1, after Kronauer, shows C_{DS}, obtained from (1), against b/a for various values of U_S/U_0. It can be seen that, for each value of U_S/U_0, C_{DS} is very insensitive to changes in b/a, the street drag coefficient passing through a broad minimum. Kronauer has proposed a new criterion for stability which states that for a given vortex velocity U_S the vortex street adjusts itself into the configuration giving minimum C_{DS}. The stability criterion can be written as

$$\left(\frac{\partial C_{DS}}{\partial(b/a)}\right)_{U_S/U_0=\text{constant}} = 0. \tag{4}$$

This stability criterion is based on no direct experimental evidence and one of the purposes of this investigation is to determine whether it predicts realistic values of the various vortex street parameters.

Many authors have attempted to formulate a universal Strouhal number to compare the wakes of various bluff bodies. The most widely used universal wake Strouhal number is that due to Roshko (1954*b*). Roshko found, however, that when a splitter plate was introduced into the wake of a circular cylinder the value of his universal Strouhal number depended on splitter plate position. The effect caused by the introduction of wake interference elements on the value of Roshko's wake Strouhal number is investigated further.

2. Measurement of the longitudinal spacing between vortices

2.1. *Experimental arrangement*

The blunt-trailing-edge models used (fully described in Bearman (1965, 1966)) had a base height h of 1 in. (2·54 cm) and chord of 6 in. (15·25 cm). The Reynolds number R_b, based on h, was in the range $1{\cdot}3 \times 10^4$ to $4{\cdot}1 \times 10^4$. The nose sections were elliptical and transition wires were attached at 20 % chord. One model had provision for fitting splitter plates and the other had a porous base through which air could be bled into the wake. In each case the shear layers leaving the body were parallel and by applying free-streamline theory it can be shown that the pressure drag coefficient, with base height as reference length, is equal to $-(C_p)_b$, the base pressure coefficient.

In Bearman (1965) measurements were presented of S and base pressure coefficient, $(C_p)_b$, against splitter plate length ℓ. Similar quantities were given in Bearman (1966), this time as a function of bleed rate C_q. $C_q = V_j d/U_0 h$, where V_j is bleed velocity and d/h is the proportion of the base that was porous. Further experiments are described here to obtain a/h as a function of ℓ/h and C_q.

2.2. *Experimental procedure and results*

The longitudinal spacing a between successive vortices of the same row was measured by using two hot wires. One wire, the reference wire, was fixed at some position in the wake while the second wire, the movable wire, could be traversed along the x-axis of the wake. The two resulting signals, after suitable filtering, were displayed on an oscilloscope, one through the X-plates and the other through the Y-plates, and exhibited the familiar Lissajou figures. To obtain the steadiest figures it was found that both wires had to be in the same spanwise plane. The upstream wire was positioned a little above the downstream one in order that there should be no interference from its wake.

Typical plots of phase relationships along the wake are shown in figure 2 for the basic model ($\ell/h = 0$ or $C_q = 0$), for the model with a splitter plate of length $1{\cdot}125h$ and for the model with a bleed quantity $C_q = 0{\cdot}0525$. x is the distance of the movable wire from the model trailing edge. The slope of the curve at any position will give the reciprocal of the longitudinal spacing of the vortices at that position. This plot shows that a becomes constant within 3 or 4 base heights of the model trailing edge. As slope decreases, spacing increases; thus near the model

the vortices were much more closely spaced. Very close to the base the signals were so weak that it was impossible to form steady Lissajou figures. As splitter plates were added, or bleed quantity increased, the distance downstream at which steady figures first appeared moved farther from the base.

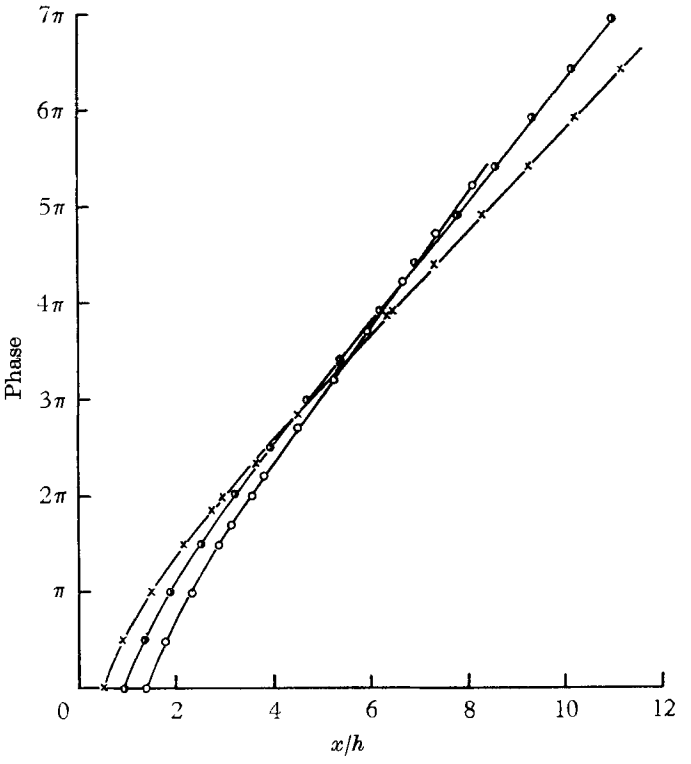

FIGURE 2. Phase relations along the wake. ×, $l/h = 0$, $R_b = 2{\cdot}3 \times 10^4$; ○, $l/h = 1{\cdot}125$, $R_b = 2{\cdot}3 \times 10^4$; ◑, $C_q = 0{\cdot}0525$, $d/h = 0{\cdot}93$, $R_b = 4{\cdot}1 \times 10^4$.

The region in which a was found to be constant will be referred to as the stable region. Figure 3 shows a plot of the stable region vortex spacing a/h versus splitter plate length for $R_b = 2{\cdot}3 \times 10^4$ and $4{\cdot}1 \times 10^4$. From the measurements there appeared to be no consistent relationship between the two Reynolds number cases, but this may have been due to inaccuracies in measuring a/h. The movable probe could be positioned to within $\pm 0{\cdot}01h$ but there was a small range of x over which the Lissajou figure was observed. This was probably caused by an unsteadiness in the basic vortex-shedding mechanism. The accuracy in measuring a/h was limited to about 2 %, but could have been worse for the $2{\cdot}0h$ splitter plate, where the velocity fluctuations associated with shedding were comparatively weak.

With knowledge of the shedding frequency and vortex spacing it was now possible to evaluate U_N, the velocity with which vortices passed the hot-wire probe:

$$U_N/U_0 = Sa/h.$$

U_N/U_0 evaluated in the stable region is shown plotted in figure 3 against ℓ/h for the two previous Reynolds number cases. The accuracy is expected to be no better than 3 %, since it depends on the accuracy of the measured values of S and

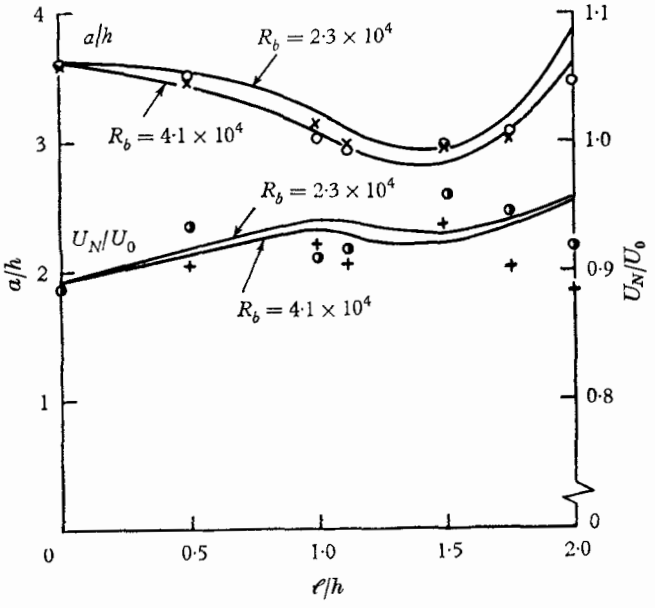

FIGURE 3. a/h and U_N/U_0 versus splitter plate length. —, potential flow model.
a/h: ×, $R_b = 2{\cdot}3 \times 10^4$, ○, $R_b = 4{\cdot}1 \times 10^4$;
U_N/U_0: ◑, $R_b = 2{\cdot}3 \times 10^4$, +, $R_b = 4{\cdot}1 \times 10^4$.

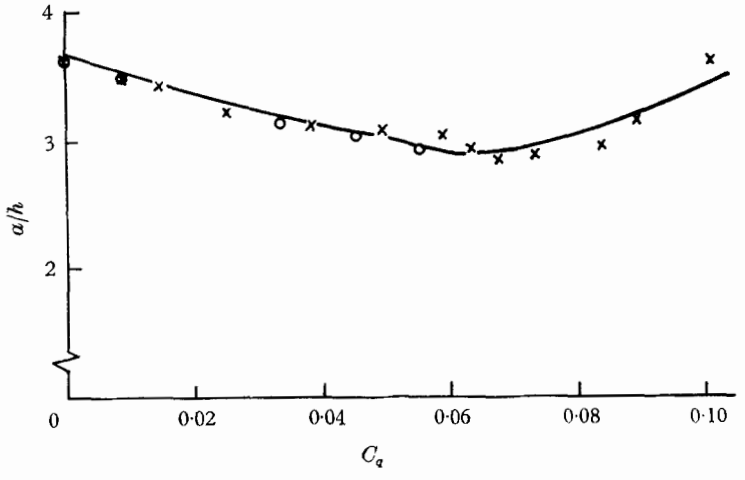

FIGURE 4. a/h versus bleed rate, $d/h = 0{\cdot}59$. —, potential flow model; ×, $R_b = 2{\cdot}3 \times 10^4$; ○, $R_b = 4{\cdot}1 \times 10^4$.

a/h. For the basic model the vortices were travelling between 88 and 89 % of free-stream velocity. Since the shedding frequency was constant down the wake it is evident from figure 2 that in the initial part of the wake the vortices were accelerating.

Plots of a/h in the stable region versus bleed rate, for the two slot widths (d/h) investigated, are shown in figures 4 and 5. The shape of these curves is very similar to the shape of the splitter plate curves in figure 3.

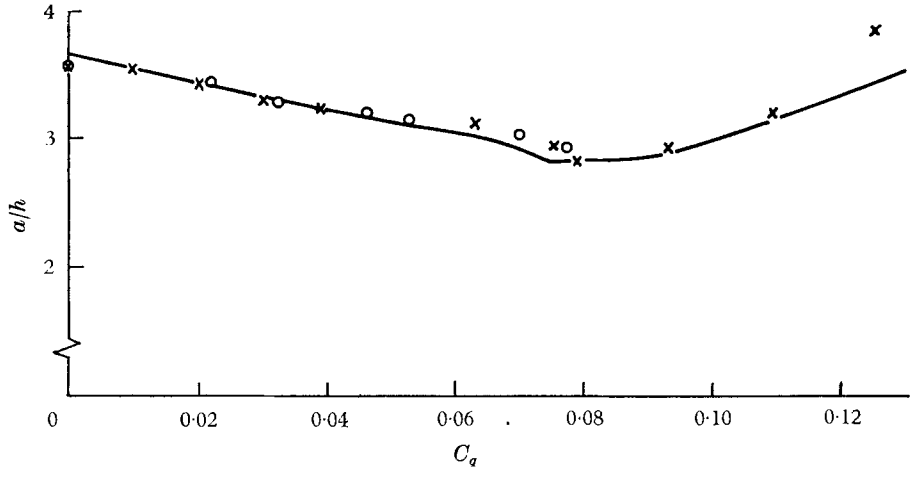

FIGURE 5. a/h versus bleed rate, $d/h = 0{\cdot}93$. —, potential flow model; ×, $R_b = 2{\cdot}3 \times 10^4$; ○, $R_b = 4{\cdot}1 \times 10^4$.

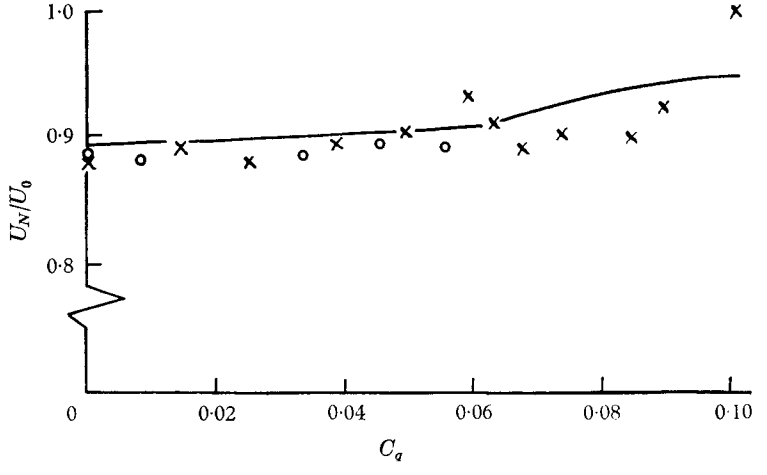

FIGURE 6. U_N/U_0 versus bleed rate, $d/h = 0{\cdot}59$. —, potential flow model; ×, $R_b = 2{\cdot}3 \times 10^4$; ○, $R_b = 4{\cdot}1 \times 10^4$.

As described in Bearman (1966), over a range of C_q, the hot-wire signals showed very regular fluctuations at frequencies associated with vortex shedding. The resulting Lissajou figures were very steady and the values of a obtained are likely to be more accurate than those found in the splitter plate investigation. In the region of C_q approaching the value where regular shedding ceased the Lissajou figures became very unsteady and hence the accuracy of a deteriorated.

Shown in figures 6 and 7 are plots of U_N/U_0 against C_q. It can be seen that there was a general trend towards higher values of U_N/U_0 with increasing bleed rate.

For the larger slot width values of U_N/U_0 greater than unity were recorded at high values of C_q. This would appear to have no meaning and is probably due to the inaccuracy in measuring a, at high values of C_q, mentioned above.

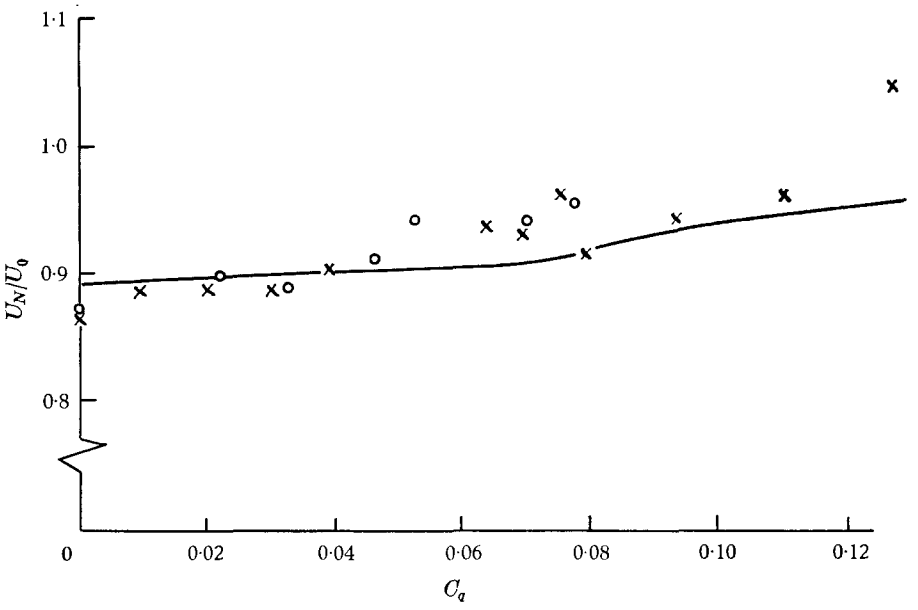

FIGURE 7. U_N/U_0 versus bleed rate, $d/h = 0{\cdot}93$. —, potential flow model; ×, $R_b = 2{\cdot}3 \times 10^4$; ○, $R_b = 4{\cdot}1 \times 10^4$.

3. Prediction of vortex street parameters

3.1. *Vortex velocity and longitudinal spacing*

In the introduction the well-known potential flow model of the wake was described and the expression (equation (1)) governing the drag associated with such a model was presented. Differentiating this equation and applying the Kronauer stability criterion (equation (4)) gives

$$2\cosh\frac{\pi b}{a} = \left(\frac{U_0}{U_S} - 2\right)\sinh\frac{\pi b}{a}\left(\cosh\frac{\pi b}{a}\sinh\frac{\pi b}{a} - \frac{\pi b}{a}\right). \tag{5}$$

The relationship between b/a and U_S/U_0 is shown plotted in figure 8 for values of U_S/U_0 up to 0·24. The von Kármán stability condition, that $b/a = 0{\cdot}281$, is also plotted in figure 8 and corresponds to a value of $U_S/U_0 = 0{\cdot}14$, which is a fairly representative value for many bluff-body shapes.

As U_S/U_0 tends to zero, b/a also tends to zero, which suggests a flow configuration consisting of a line of equal, contra-rotating vortices advancing with zero velocity relative to the free stream. The circulation associated with an individual vortex and the drag of such an array can be shown, from (1), to go to zero. The other extreme condition of (5) is when b/a tends to infinity and then

$$\cosh(\pi b/a) \approx \sinh(\pi b/a) \quad \text{and} \quad \cosh(\pi b/a)\sinh(\pi b/a)$$

becomes very much greater than $\pi b/a$. Thus (5) becomes

$$\frac{U_0}{U_S} - 2 = \frac{2}{\cosh(\pi b/a)\sinh(\pi b/a)} \to 0 \tag{6}$$

and therefore $U_S = \frac{1}{2}U_0$. This describes the flow in two shear layers where each shear layer is represented by a line of very closely spaced point vortices, such that the distance between the shear layers is very much greater than the longitudinal spacing between successive vortices. Between these two extremes lies the range of values of b/a for which vortex streets are formed.

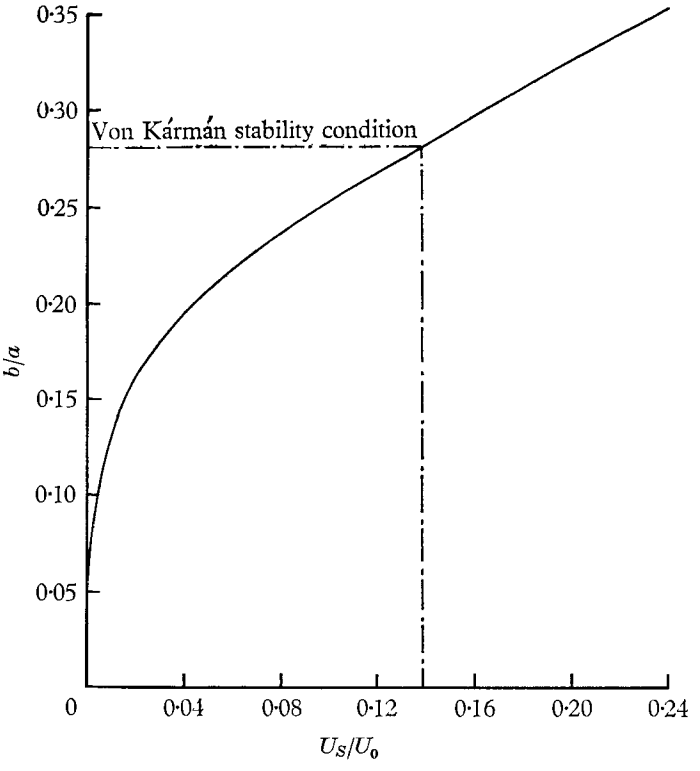

FIGURE 8. b/a versus U_S/U_0 for the condition C_{DS} is a minimum.

For each value of U_S/U_0 there is a corresponding value of b/a which makes C_{DS} a minimum. The minimum vortex street drag coefficient, C_{DSM}, is shown plotted in figure 1 against a limited range of values of b/a.

The vortex street drag force can be equated to a drag force experienced by the body. The problem arises, however, as to whether the vortex street drag should be equated to the body pressure drag or profile drag. With most bluff-body shapes skin friction represents a small contribution to total drag. With the basic blunt-trailing-edge section described here skin friction accounted for about 15 % of the total drag. This percentage contribution rose to about 30 % when a $2h$ splitter plate was added. The assumption made here is that vortex street drag, derived

from the idealized potential flow model of the wake, should be equated to body pressure drag.

In Bearman (1965, 1966) the effects of wind tunnel blockage on the model drag and base pressure were estimated using the Maskell (1965) correction. This method is only valid, however, up to the position in the wake at which the shear layers become parallel, and no detailed information is known about the effects of blockage on the vortex street itself. The drag of the model is to be equated to the drag of the vortex street and thus to be consistent only measured values will be compared.

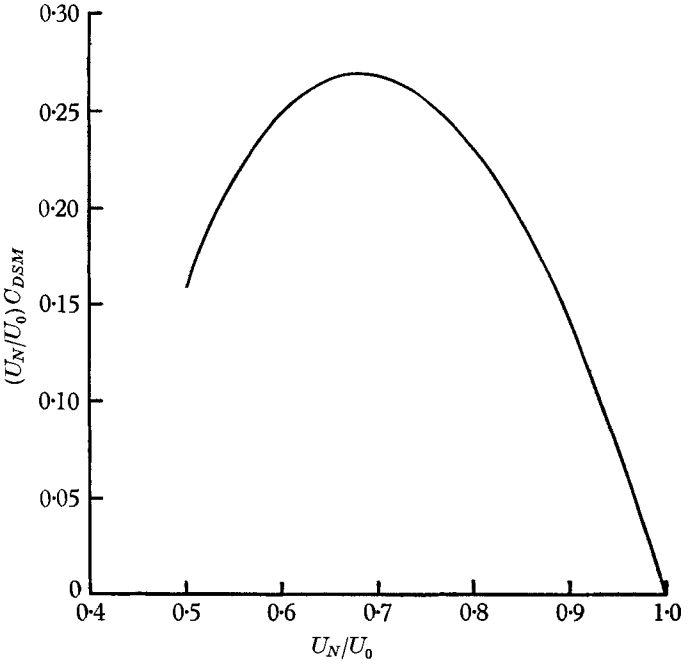

FIGURE 9. $(U_N/U_0)\,C_{DSM}$ versus U_N/U_0.

The body pressure drag coefficient, C_{DF}, can be related to the drag coefficient of the vortex street by

$$hC_{DF} = aC_{DS}, \tag{7}$$

where $C_{DF} = D_F/\frac{1}{2}\rho U_0^2 h$ and D_F is the body pressure drag force. Multiplying (7) by S gives

$$SC_{DF} = S\frac{a}{h}C_{DS} = \frac{U_N}{U_0}C_{DS} = F\left(\frac{U_N}{U_0}\right). \tag{8}$$

If either the von Kármán or the Kronauer stability criterion is used to evaluate C_{DS} the product SC_{DF} is only a function of the velocity of the vortices. Figure 9 shows a plot of $(U_N/U_0)\,C_{DSM}$ against U_N/U_0, where C_{DSM} was obtained using the Kronauer stability criterion. Thus using this plot it is possible to predict U_N/U_0 from measured values of S and C_{DF}. In the following, unless otherwise stated, the Kronauer stability criterion will be used to determine U_N/U_0.

It has been shown that, as U_N/U_0 tends to 0·5, b/a tends to infinity and therefore all possible values of U_N/U_0 must be greater than 0·5. It can be seen from figure 9

that there are two possible solutions of U_N/U_0 for values of $(U_N/U_0)C_{DSM}$ greater than 0·16. It is assumed that the greater of the two solutions always exists, which means that vortex velocities must be greater than about $0{\cdot}70U_0$. Fage & Johansen (1927) measured U_N/U_0 for a large variety of bluff-body shapes and the smallest value recorded was $0{\cdot}77U_0$. The author knows of no measurements in a fully developed vortex street where U_N/U_0 was less than 0·70.

Predicted values of U_N/U_0 are shown compared with those measured in the base bleed experiments in figures 6 and 7 for $d/h = 0{\cdot}59$ and 0·93 respectively. The theory appears to show the general trend of the results quite well and the agreement is particularly good up to a value of C_q of about 0·05. If the theoretical value of U_N/U_0 is divided by the experimental value of S corresponding to that particular C_q, a value for a/h is found. These values are shown in figures 4 and 5 and the agreement between theory and experiment is again close.

The splitter plate results are shown in figure 3 for the two Reynolds number cases. The agreement between the theoretical and experimental values was not so good; the curve of U_N/U_0 has an opposite slope to the experimental results for long splitter plates. The reasons for this may lie in the inaccuracy of the experimental results for values of ℓ/h greater than 1·75. The shedding frequency for these long splitter plates was not sharply defined and it may well have been more appropriate to represent S by a band of possible values, corresponding to a band of values for U_N/U_0. The values of a/h obtained with the splitter plates are again fairly well predicted by the potential flow model.

The drag of the potential vortex street model, as shown by figure 9, is extremely sensitive to changes in U_N/U_0. The drag formula (1) is a function of U_S/U_0 and since U_N/U_0 is often near unity it is very difficult to measure U_S/U_0 very accurately. Taking the basic model as an example: if U_N/U_0 changes by 1 %, Strouhal number remaining constant, C_{DF} changes by 8 %. It is not possible, therefore, within the limits of experimental accuracy, to measure a/h and S and hope to predict accurate values of C_{DF}. It can be seen that the vortex street parameters need only change very slightly to accommodate large changes in drag. On the other hand, this means that, if drag and Strouhal number are known, accurate values of U_N/U_0 and a/h can be predicted.

3.2. *Lateral spacing and spacing ratio*

As shown by Kronauer (1964) the spacing ratio is not an important parameter in the determination of drag and hence the von Kármán drag formula (2) would have predicted the values of U_N/U_0 and a/h equally well. The foregoing work serves to show, however, that the vortex street model predicts realistic values in vortex streets with and without wake interference. Use of the Kronauer stability criterion allows additional predictions to be made of spacing ratio, and also b/h, which may be more representative of the actual flow than those found by using the von Kármán condition, $b/a = 0{\cdot}281$.

Figure 10 shows estimations of b/h and b/a for the splitter plate results at $R_b = 2{\cdot}3 \times 10^4$; suffix v denotes the von Kármán stability criterion has been used and suffix k the Kronauer criterion. Figure 11 shows the corresponding quantities derived from the base bleed results with $d/h = 0{\cdot}93$. It is interesting to note that,

for the bleed case, the Kronauer values of b/a were almost constant up to $C_q = 0{\cdot}07$. This corresponds to the C_q at which S was a maximum and where there was a kink in the base pressure versus C_q curve described in Bearman (1966). In

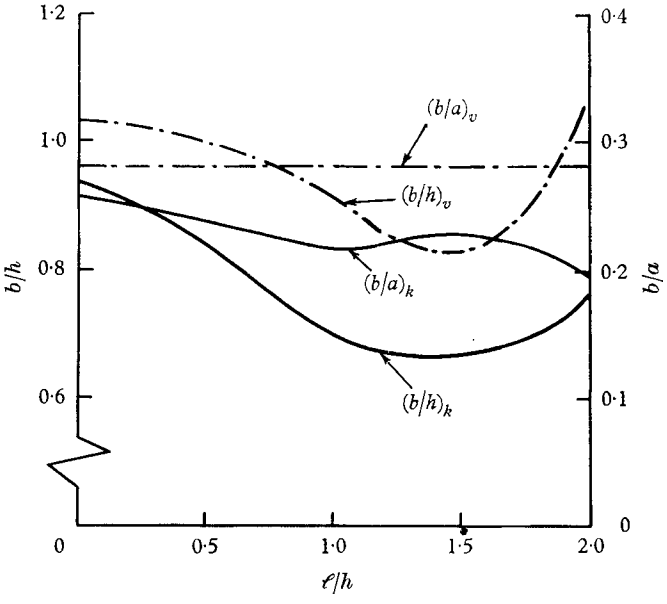

FIGURE 10. Splitter plates—estimation of b/a and b/h at $R_b = 2{\cdot}3 \times 10^4$.

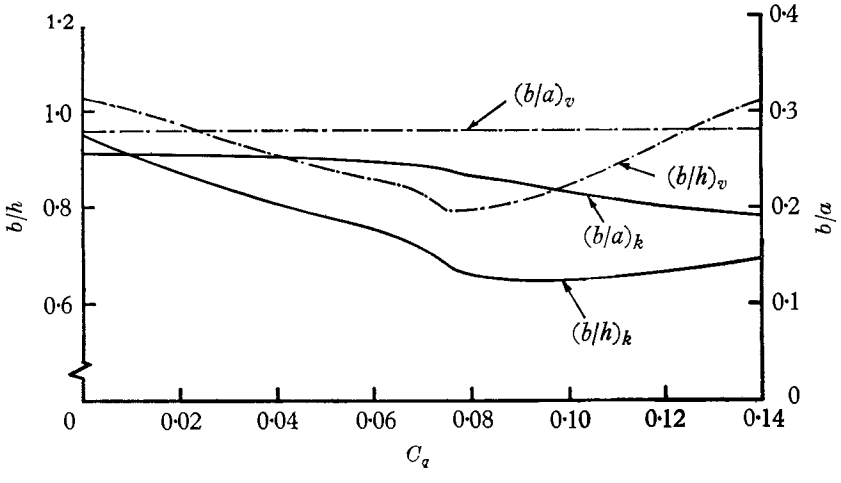

FIGURE 11. Base bleed—estimation of b/a and b/h, $d/h = 0{\cdot}93$.

all cases the von Kármán stability criterion predicted higher values of b/h but the shapes of the curves were very similar.

It is very difficult to determine b/h experimentally. Berger (1964) states that no characteristic hot-wire signal can be expected from the centres of vortices and criticizes measurements of b/h that have been obtained by the 'hot-wire technique'. In an attempt to estimate b/h the flow in the wake of the base bleed model

was visualized with smoke. At high Reynolds numbers it proved very difficult to locate the centres of vortices and the only conclusion was that b/a appeared to be less than 0·281 but that it was impossible to assign an accurate value to it. This in itself, therefore, offers very little proof that $(b/h)_k$ is more representative than $(b/h)_v$. It is proposed, by the introduction of a new universal Strouhal number, to substantiate that $(b/h)_k$ is more representative than $(b/h)_v$.

3.3. *Wake Strouhal number*

It was demonstrated by Roshko (1954*b*) that, by applying simple physical arguments to the mechanism of vortex shedding, a parameter could be derived to compare the wakes of different bluff bodies. He considered two shear layers a distance h' apart with the velocity outside the layers equal to U_b, the velocity at the edge of the boundary layer at the separation point. The frequency with which vortices were formed was considered proportional to U_b/h' and thus a wake Strouhal number S_R could be formed where

$$S_R = fh'/U_b.$$

By applying Bernoulli's equation to the flow at the separation point, just outside the boundary layer,

$$U_b = U_0[1-(C_p)_b]^{\frac{1}{2}}.$$

It is convenient to replace $[1-(C_p)_b]^{\frac{1}{2}}$ by K and then

$$S_R = Sh'/Kh.$$

h' was obtained by the notched hodograph method (Roshko 1954*a*) for three simple geometric shapes: circular cylinder, flat plate and 90° wedge. This gave a fairly constant S_R of $0{\cdot}163 \pm 0{\cdot}01$ over most of the Reynolds number range examined.

The notched hodograph method gives the spacing of the shear layers when they become parallel and it is assumed that the vortices begin to form from shear layers with this spacing. With the model shape used to obtain the results described in this paper $h' = h$ and thus $S_R = S/K$. For the basic model this gave a value of $S_R = 0{\cdot}19$. With the introduction of wake interference it has been shown (see Bearman 1966) that the vortex formation position is moved farther from the body. Thus, although h' still equals h, it is no longer representative of the distance between shear layers at the commencement of shedding. For example, at $C_q = 0{\cdot}08$ and $d/h = 0{\cdot}93$, $S_R = 0{\cdot}278$ and thus S_R appears unsuitable for comparing the wakes of bluff bodies with wake interference.

The typical length required will be called h'' and is the distance between shear layers at the commencement of vortex shedding. If the assumption is now made that the lateral displacement b between the vortex rows is equal to h'', a new Strouhal number is obtained. The new Strouhal number S_B becomes

$$S_B = fb/U_b = Sb/Kh.$$

S and K are measured values and b/h can be found by using either the von Kármán or the Kronauer stability criterion. S_B, found by using the Kronauer stability condition, is plotted against K in figure 12 for the splitter plate and base bleed

results, and over the majority of the range a constant value of S_B of about 0·181 was obtained. At low values of K, corresponding to high C_q and long splitter plates, there was a slight reduction in S_B. This was not surprising because it can be shown that, when $K = 1$, S_B will be zero. Taking as an example the basic model shape, it is seen that when $K \to 1$ (i.e. $(C_p)_b \to 0$) $C_{DF} \to 0$. Therefore the vortex street drag will tend to zero and $U_N/U_0 \to 1$, which means that the spacing ratio will approach zero. Now since

$$S_B = \frac{fb}{U_b} = \frac{fb}{U_b}\frac{U_0}{U_0}\frac{a}{a} = \frac{U_N}{U_0}\frac{b}{a}\frac{1}{K}$$

it is clear that S_B will tend towards zero. This suggests that the length scale b is not universal and that at low values of K some other length may be more appropriate. This point is returned to later. In the experiments it was found that the wake stabilized and shedding ceased long before $S_B = 0$.

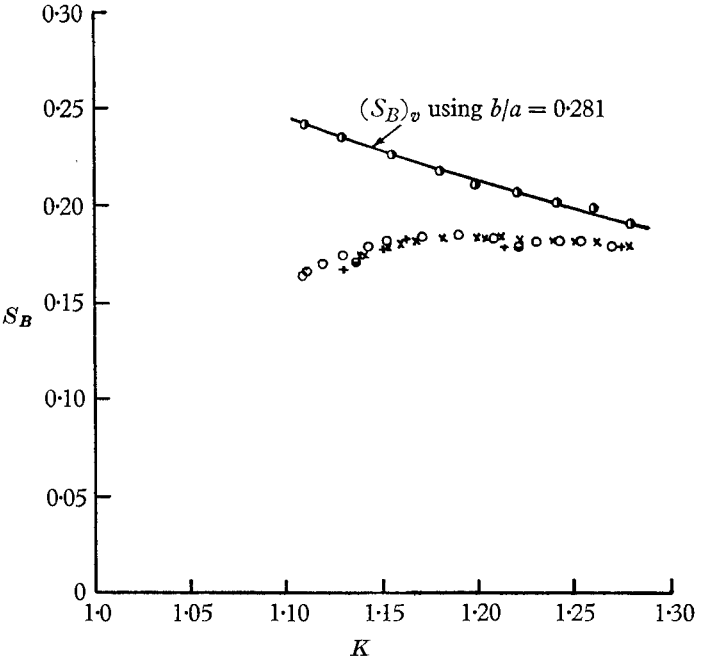

FIGURE 12. Universal Strouhal number S_B versus K for the base bleed and splitter plate results. ×, bleed $d/h = 0{\cdot}59$; ◑ and ○, bleed $d/h = 0{\cdot}93$; +, splitter plates $R_b = 2{\cdot}3 \times 10^4$; ◒, splitter plates $R_b = 4{\cdot}1 \times 10^4$.

If the von Kármán stability criterion had been used to predict b/h a constant value of S_B would not have been obtained. This is demonstrated in figure 12, where $(S_B)_v$ decreases with increasing K. Since S_B involves parameters characteristic of the wake the existence of a constant value of S_B would appear to place some justification on the validity of the Kronauer stability criterion. As a more rigorous test the analysis has been extended to a variety of bluff-body shapes.

For an arbitrary shape the information required to compute S_B are the values of C_{DF}, $(C_p)_b$ and S. Many investigators have examined circular cylinders over the Reynolds number range $R_b = 10^2$ to 10^5. The results used here are mainly

taken from Roshko (1954*b*) and Relf & Simmons (1924). Roshko (1961) has carried out experiments at higher Reynolds numbers ($R_b = 2 \times 10^6$ to 10^7) where the boundary layers on the cylinder were turbulent. Flat plate and 90° wedge data have been obtained from Roshko (1954*b*). Further base bleed data were taken from Wood (1964) and Bellhouse & Wood (1965). Fage & Johansen (1927) have published results for an ogival and extended ogival shape and Nash, Quincey &

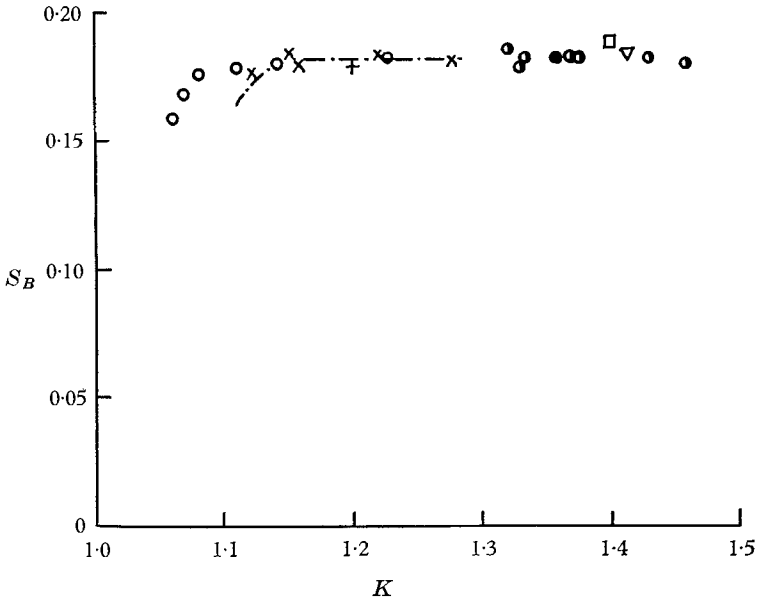

FIGURE 13. Universal Strouhal number S_B versus K for various bluff-body shapes. ×, splitter plates, Nash *et al.* (1963) Mach no. 0·4; ○, base bleed, Wood (1964) and Bellhouse & Wood (1965); ◒, ogival shape, Fage & Johansen (1927); +, extended ogival shape, Fage & Johansen (1927); ▽, 90° wedge, Roshko (1954*b*); □, flat plate, Roshko (1954*b*); ◑, circular cylinder, $R = 10^2$ to 10^5; ●, circular cylinder, $R = 2 \times 10^6$ to 10^7, Roshko (1961); —·—·, mean of results from figure 12.

Callinan (1963) have presented results for a bluff section fitted with splitter plates. The last two authors only present $(C_p)_b$ and S but in each case the shear layers left the model parallel and free streamline theory has been applied to obtain C_{DF}. The values of S_B for these various bodies are plotted in figure 13 and again show a collapse of the data on to a value of $S_B = 0{\cdot}181$.

A given value of $C_{DF}S$, assuming a universal Strouhal number S_B, implies a given value of K. $C_{DF}S$ is shown plotted against K in figure 14 for all the available data and shows a reasonable collapse of the results. The curve shown in figure 14 was obtained by assuming the Kronauer stability criterion to hold and putting $S_B = 0{\cdot}181$. The scatter shown in figure 14 would have been greater if profile drag coefficient instead of C_{DF} had been used.

Goldberg & Florsheim (1966) have proposed a universal Strouhal number S_θ using the total wake momentum thickness θ as the relevant characteristic length. They define $S_\theta = f\theta/U$ and show that, for a two-dimensional body, $\theta/h = \frac{1}{2}C_D$, where C_D is profile drag coefficient, and $S_\theta = \frac{1}{2}SC_D$. For bluff bodies $C_D \approx C_{DF}$

and thus figure 14 represents a plot of $2S_\theta$ against K. Clearly S_θ is not universal but is related to base pressure. Gerrard (1966) also showed that S_θ is not a universal Strouhal number.

Although figure 14 shows a general collapse of the data it does not take account of the detailed variations of S, C_{DF} and $(C_p)_b$ at low values of K. As in figure 12 the bleed and splitter plate results show a trend away from the curve $S_B = 0{\cdot}181$ for values of K less than about 1·16. This value of base pressure corresponds to the

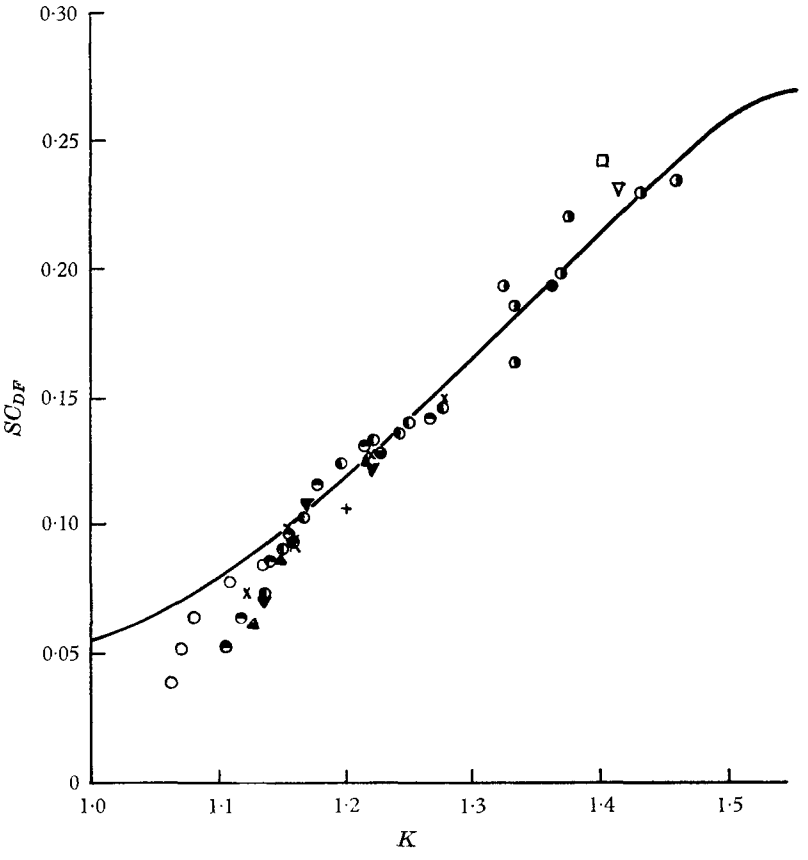

FIGURE 14. SC_{DF} versus K for various bluff-body shapes. ▲, splitter plates, $R_b = 2{\cdot}3 \times 10^4$; ▼, splitter plates, $R_b = 4{\cdot}1 \times 10^4$; ◐, base bleed $d/h = 0{\cdot}59$; ◓, base bleed $d/h = 0{\cdot}93$; other symbols as figure 13; —, assuming $S_B = 0{\cdot}181$.

value of C_q and ℓ/h at which S was a maximum. Wood's results also show a trend away from the line $S_B = 0{\cdot}181$ for values of K less than 1·09. This value of K also corresponds to the C_q at which S was a maximum. As K approaches 1, $C_{DF}S$ approaches zero and, in view of the fact that S_B must go to zero as K goes to 1, noted earlier, the trend of the experimental data in figure 14 appears significant. Again this demonstrates that the idea of a constant S_B breaks down as $K \to 1$ and that some other length scale becomes important. Further research is required to determine if there is a change in the vortex formation process at these low values of K.

4. Summary of methods of predicting vortex street parameters

It may prove useful to summarize the methods used to estimate the various vortex street parameters. The basic model adopted is the von Kármán potential flow model of the vortex street wake. This model is used in conjunction with the proposal by Kronauer (1964) that the vortex street spacing, for a given vortex velocity, adjusts itself into a configuration giving a minimum vortex street drag coefficient C_{DSM}, where C_{DSM} is based on longitudinal vortex spacing a.

Given the measured values of Strouhal number and pressure drag coefficient it is possible to determine U_N/U_0 from figure 9 since $SC_{DF} = (U_N/U_0)C_{DSM}$. The longitudinal vortex spacing is determined, knowing U_N/U_0, from the relation $Sa/h = U_N/U_0$. Once U_N/U_0 is known b/a can be determined through the unique relationship, shown in figure 8, between vortex velocity and spacing ratio. The value of the lateral spacing of the vortices follows. The only significant difference found using the Kronauer, in place of the von Kármán, stability criterion is in the estimation of the lateral spacing b and hence spacing ratio.

The new universal Strouhal number, $S_B = fb/U_b$, has been derived by following similar arguments to those put forward by Roshko (1954*b*). The characteristic length, however, is taken as the lateral displacement b between vortex rows instead of the shear layer spacing h' obtained by the notched hodograph method. b is obtained as outlined above and U_b is simply related to base pressure. The relationship between Strouhal number times pressure drag coefficient and the base pressure parameter K, shown in figure 14, was suggested from the definition of S_B. By using this correlation of results the vortex-shedding frequency of a bluff body can be determined from its pressure distribution.

5. Conclusions

The von Kármán vortex street drag formula was found to predict accurate values of the velocity of vortices and the longitudinal spacing between vortices, in wakes with splitter plates and base bleed. Both the von Kármán and Kronauer stability criteria were used to estimate the lateral spacing b between vortices. It was not possible to compare directly these estimates of b with measured values.

The value of Roshko's universal wake Strouhal number was affected by the introduction of wake interference elements. Using the Kronauer stability condition to determine b, a new universal wake Strouhal number was formed: $S_B = fb/U_b$. When plotted against the base pressure parameter K, $S_B = 0{\cdot}181$ over a wide range of K for a variety of bluff-body shapes. It is thought that this justifies, in part, the use of the Kronauer stability criterion.

An analysis of results from different bluff-body shapes has shown that a correlation exists between the product $C_{DF}S$ and the base pressure parameter K.

The work described in this paper was undertaken in the Aeronautics Sub-Department of the Cambridge University Engineering Laboratory. The research was supervised by Dr D. J. Maull, whose helpful advice and continual encouragement are gratefully acknowledged.

The author was in receipt of a maintenance grant from the Science Research Council.

REFERENCES

BEARMAN, P. W. 1965 *J. Fluid Mech.* **21**, 241–255.

BEARMAN, P. W. 1966 *Agard C.P.* no. 4, *Separated Flows*, pp. 479–508.

BELLHOUSE, B. J. & WOOD, C. J. 1965 *J. R. Aero. Soc.* **69**, 789–791.

BERGER, E. 1964 *Z. Flugwiss.* **12**, 41–59.

FAGE, A. & JOHANSEN, F. C. 1927 *Aero. Res. Coun. Lond. R. & M.* no. 1143.

GERRARD, J. H. 1966 *J. Fluid Mech.* **25**, 401–413.

GOLDBURG, A. & FLORSHEIM, B. H. 1966 *Phys. Fluids* **9**, 45–50.

KRONAUER, R. E. 1964 *Predicting eddy frequency in separated wakes.* Paper presented at the I.U.T.A.M. symposium on concentrated vortex motions in fluids, University of Michigan, Ann Arbor, Michigan, 6–11th July.

MASKELL, E. C. 1965 *Aero. Res. Coun. Lond. R. & M.* no. 3400.

MILNE-THOMSON, L. M. 1938 *Theoretical Hydromechanics.* London: Macmillan.

NASH, J. F., QUINCEY, V. G. & CALLINAN, J. 1963 *Aero. Res. Counc., Lond. Rept.* no. 25,070.

RELF, E. F. & SIMMONS, L. F. G. 1924 *Aero. Res. Coun., Lond. R. & M.* no. 917.

ROSHKO, A. 1954*a* *Nat. Adv. Comm. Aero. Wash. Tech. Note*, no. 3168.

ROSHKO, A. 1954*b* *Nat. Adv. Comm. Aero. Wash. Tech. Note*, no. 3169.

ROSHKO, A. 1961 *J. Fluid Mech.* **10**, 345–356.

TIMME, A. & WILLE, R. 1957 *Jb. schiffbautech. Ges.* **51**, 215–221.

WILLE, R. 1960 *Advanc. appl. Mech.* **6**, 273–287.

WOOD, C. J. 1964 *J. R. Aero. Soc.* **68**, 477–482.